Electronic Journal of Biotechnology 77 (2025) 12–23

Contents lists available at ScienceDirect

Electronic Journal of Biotechnology

journal homepage: www.elsevier.com/locate/ejbt

Research article

Onion peel-mediated biosynthesis of TiO_2-ZnO bimetallic nanoparticles: Antimicrobial, antibiofilm, and anticancer activities ☆

Ebrahim Saied [a,*], Ahmed S. Doghish [b,c], Mohamed K.Y. Soliman [a], Walaa A. El-Dakroury [d], Abeer S. Aloufi [e], Bushra Hafeez Kiani [f], Amr H. Hashem [a,*]

[a] Botany and Microbiology Department, Faculty of Science, Al-Azhar University, Nasr City, Cairo, Egypt
[b] Department of Biochemistry, Faculty of Pharmacy, Badr University in Cairo, Badr City, Cairo, Egypt
[c] Biochemistry and Molecular Biology Department, Faculty of Pharmacy (Boys), Al-Azhar University, Nasr City, Cairo, Egypt
[d] Department of Pharmaceutics and Industrial Pharmacy, Faculty of Pharmacy, Badr University in Cairo, Badr City, Cairo, Egypt
[e] Department of Biology, College of Science, Princess Nourah bint Abdulrahman University, Riyadh, Saudi Arabia
[f] Department of Biology and Biotechnology, Worcester Polytechnic Institute, Worcester, MA, USA

GRAPHICAL ABSTRACT

Onion peel-mediated biosynthesis of TiO_2-ZnO bimetallic nanoparticles: Antimicrobial, antibiofilm, and anticancer activities.

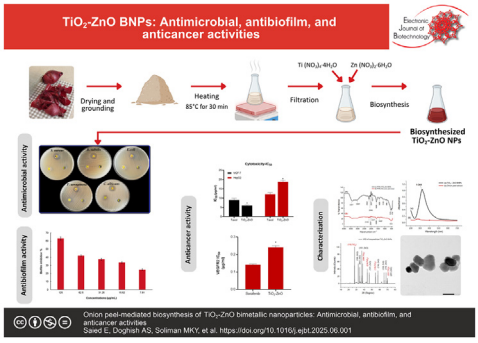

ARTICLE INFO

Article history:
Received 15 February 2025
Accepted 11 June 2025
Available online 7 August 2025

Keywords:
Antibiofilm
Anticancer
Antimicrobial
Bimetallic nanoparticles
Biomedical applications
Green biosynthesis

ABSTRACT

Background: The rising challenges of antibiotic resistance and cancer necessitate the development of sustainable, cost-effective, and multifunctional therapeutic agents. This study introduces a green synthesis approach for bimetallic nanoparticles (BNPs) using agro-waste materials.
Results: For the first time, bimetallic titanium dioxide–zinc oxide (TiO_2-ZnO) BNPs were synthesized using onion peel extract as a natural reducing and stabilizing agent. UV–Vis spectroscopy confirmed nanoparticle formation with a peak corresponding to a size of approximately 320 nm. DLS showed an average hydrodynamic diameter of 145.1 nm, and TEM revealed monodispersed nanoparticles, ranging from 80 to 150 nm. The BNPs exhibited broad-spectrum antimicrobial activity with MIC values of 500 µg/mL against *Bacillus subtilis*, *Pseudomonas aeruginosa*, and *Candida albicans*; 1000 µg/mL against *Staphylococcus aureus*; and 250 µg/mL against *Escherichia coli*. They also demonstrated significant antibiofilm activity against *B. subtilis*-MRSA with a 63.1% inhibition rate at 125 µg/mL. Additionally, TiO_2-ZnO

☆ Audio abstract available in Supplementary material.
Peer review under responsibility of Pontificia Universidad Católica de Valparaíso.
* Corresponding authors.
E-mail addresses: hema_almassry2000@azhar.edu.eg (E. Saied), amr.hosny86@azhar.edu.eg (A.H. Hashem).

https://doi.org/10.1016/j.ejbt.2025.06.001

Nanomaterials
Nanoplatform
Onion peel
Titanium dioxide–zinc oxide

BNPs showed potent cytotoxic effects on MCF-7 breast cancer cells, with an IC_{50} of 5.97 ± 0.37 μg/mL, and anticancer activity was mediated by caspase-8 activation and VEGFR-2 downregulation.
Conclusions: This green-synthesized TiO_2-ZnO BNPs offer a promising dual-function nanoplatform for combating microbial infections and cancer, highlighting the potential of sustainable nanotechnology for biomedical applications.

How to cite: Saied E, Doghish AS, Soliman MK, et al. Onion peel-mediated biosynthesis of TiO_2-ZnO bimetallic nanoparticles: Antimicrobial, antibiofilm, and anticancer activities. Electron J Biotechnol 2025;77. https://doi.org/10.1016/j.ejbt.2025.06.001.

1. Introduction

Nanotechnology is the manipulation of matter on an atomic or molecular scale, typically below 100 nm. It holds the potential to revolutionize various fields, including medicine, electronics, and materials science, by enabling the development of new materials and devices with enhanced properties [1]. Among the several categories of nanoparticles, metal-based nanoparticles, especially those composed of noble metals, have unique benefits compared to other varieties. These nanoparticles exhibit exceptional stability, biocompatibility, and scalability, rendering them suitable for biomedical and environmental applications [2]. Notwithstanding these beneficial attributes, the use of metal-based nanoparticles encounters obstacles, including concerns regarding toxicity, dimensions, cellular absorption, and chemical stability [3,4]. To mitigate these restrictions, a possible strategy involves the amalgamation of two metals to produce bimetallic nanoparticles. This combination can generate distinctive synergy among the metals, augmenting their structural and physical characteristics, and expanding their overall usefulness and prospective uses [5]. Experimental results have demonstrated that bimetallic nanoparticles can significantly outperform monometallic ones, overcoming the limitations associated with the latter.

In recent years, bimetallic nanoparticles have attracted considerable attention owing to their distinctive physical features, including quantum effects, elevated surface area, and improved mobility. These nanoparticles have enhanced chemical, mechanical, thermal, optical, catalytic, and magnetic characteristics [6,7,8]. These characteristics differentiate bimetallic nanoparticles from their monometallic counterparts, providing enhanced performance that individual metals cannot offer [9].

The widespread misuse and overdependence on antibiotics have driven the development of resistant bacterial strains, representing a significant threat to global public health. These resilient microbes have developed advanced strategies to resist antimicrobial drugs, rendering formerly effective treatments ineffectual [10,11]. As bacterial infections become increasingly harder to treat, the risk of complications from routine medical procedures rises considerably [12]. This disturbing trend jeopardizes our ability to combat both common and severe illnesses, from skin infections to pneumonia to sepsis. Without immediate and coordinated action to reduce inappropriate antibiotic usage and to innovate new antimicrobial therapies, we may face a future where even minor injuries and infections become potentially fatal [13,14]. Tackling antibiotic resistance demands a unified global response to preserve the effectiveness of essential medications and protect the health of future generations.

Although various cancer therapies, such as chemotherapy and surgical procedures, have been developed, they often result in significant adverse effects [15,16]. Thus, the primary focus of research in this discipline revolves around developing innovative techniques or anticancer drugs that exhibit enhanced efficacy, low toxicity, exceptional biocompatibility, and biodegradability. Considering all these considerations, nanotechnology is emerging as a crucial, promptly growing discipline that is making substantial progress in medication delivery, bioavailability, imaging, and chemotherapy. Moreover, it has proven effective in mitigating the side effects typically associated with conventional treatment methods [17].

The pursuit of eco-friendly and sustainable methods of nanoparticle synthesis has led researchers toward the extraordinary potential of plant-based materials [18]. Specifically, the humble peels of common fruits and vegetables have emerged as versatile templates to serve the green production of metal and metal oxide nanoparticles [19,20]. Through bioreduction and natural templating processes, the phytochemicals and biomolecules present in these plant-derived wastes can mediate the assembly of nanostructures with precisely controlled size, shape, and composition [21]. This bioinspired strategy offers significant advantages over conventional chemical synthesis routes, eliminating the need for hazardous reagents while leveraging renewable, biodegradable resources. The resulting nanoparticles have shown immense promise in diverse applications, from antimicrobial coatings to drug delivery systems, catalysts to optoelectronics [22]. Utilizing nature's inherent capabilities, scientists are pioneering a new era of environmentally benign nanomaterial production, creating a pathway to a more sustainable technological landscape.

Titanium dioxide (TiO_2) nanoparticles are in fact widely desired for a variety of applications due to their unique combination of properties. As a semiconductor, TiO_2 exhibits remarkable chemical stability and superior optoelectronic characteristics [23]. Different preparation techniques may be used to synthesize TiO_2 nanoparticles in different forms, including nanorods, nanowires, and nanotubes, which increases the versatility of their uses [24]. Their photocatalytic capabilities are especially noteworthy, enabling their use in disciplines such as environmental remediation, energy conversion, and biomedicine [25]. Similarly, zinc oxide nanoparticles are indeed distinctive, and scientists from a wide range of disciplines are interested in them. These include high electroactivity, excellent optoelectronic performance, and a strong antimicrobial potential. ZnO nanoparticles can be synthesized using methods such as precipitation, laser ablation, and thermal decomposition [26].

Several categories of metallic nanoparticles (MNPs) have been synthesized via green methods, which exhibit improved biomimetic properties. For example, gold (Au) nanoparticles have been synthesized using flower extracts of *Carthamus tinctorius* L. (safflower) and *Helianthus annuus* (sunflower), showing promising biological activities [27,28]. Silver (Ag) nanoparticles have also been reported with excellent antimicrobial properties [29]. Moreover, zinc oxide and copper (Cu) nanoparticles have demonstrated significant catalytic and antimicrobial properties [30], while iron (Fe) and palladium Pd nanoparticles have shown efficient catalytic activity [31]. These studies underscore the potential of green syn-

thesis in enhancing the functional properties of metallic NPs for various biomedical and environmental applications.

Traditional chemical and physical methods for synthesizing nanomaterials are often costly, energy-intensive, and environmentally harmful [32,33]. In contrast, green synthesis offers a safer, eco-friendly, and more economical alternative by using biological sources like plants or microorganisms. Plants, in particular, serve as both reducing and stabilizing agents, and their phytochemicals (such as flavonoids, alkaloids, and polyphenols) aid in nanoparticle formation [34]. Various plant parts (leaves, fruits, roots, and seeds) have been successfully used to produce bimetallic nanoparticles (e.g., Ag–Au, Cu–Ag, Ni/Fe_3O_4) with applications in antimicrobial, catalytic, and sensing fields [6,35]. Additionally, bio-waste such as fruit peels, leaves, and agro-waste has emerged as a valuable resource for nanoparticle synthesis, offering a dual benefit of waste reduction and nanoparticle production [36]. For instance, pomegranate peels, orange peels, and silkworm cocoons have been used to create nanoparticles with applications in dye degradation, antibacterial treatments, and cancer therapy [37]. Despite some limitations, green and waste-based synthesis remains a promising approach in developing sustainable nanomaterials [38,39]. Global onion output has increased by 25% in the last ten years, and it currently stands at 83 million tons. Because of this high level of output, the European Union only disposes of over fifty thousand tons of onion skin trash yearly [40]. Finding a suitable method of recycling the substantial quantity of solid waste produced by onion processing is a problem for the environment. Effective solid waste management is recognized as a primary problem of the twenty-first century as well as is seen as a crucial element of achieving sustainable growth [41].

In the quest for sustainable biomedical solutions, this work introduces a green synthesis strategy for producing TiO_2-ZnO BNPs using onion peel extract, an abundant agro-waste resource, as a natural reductant and stabilizer. This environmentally conscious method avoids hazardous chemicals and contributes to waste valorization. What sets this study apart is the dual functional evaluation of the synthesized nanoparticles, combining antimicrobial and antibiofilm testing with anticancer analysis an approach rarely reported in previous literature using onion peel-based systems. Furthermore, the study investigates underlying biological mechanisms by examining caspase-8 activation and VEGFR-2 expression, offering insight into their potential therapeutic pathways. The aim of this study is to develop a sustainable and cost-effective method for synthesizing TiO_2-ZnO BNPs using onion peel extract. This research seeks to evaluate the multifunctional therapeutic potential of these nanoparticles against antibiotic-resistant bacteria and breast cancer cells.

2. Material and methods

2.1. Chemicals and reagents

In Giza, Egypt, onion peels were gathered from a nearby market in 6th of October City. Zinc nitrate hexahydrate ($Zn(NO_3)_2{\cdot}6H_2O$), titanium nitrate tetrahydrate ($Ti(NO_3)_4{\cdot}4H_2O$), and NaOH were acquired from Sigma-Aldrich, Cairo, and used as precursors and a precipitating agent, respectively.

2.2. Preparation of onion peel extract

Fifty grams of red onion were washed twice with distilled water (DW) to ensure dust-free surfaces, then finely chopped and manually ground using a pestle and mortar. Heating was carried out at 85°C for the solution for 30 min with the addition of 100 mL of double-DW. The generated solution underwent filtration with Whatman No. 1 filter paper [42]. Afterward, the filtrate was diluted to a final volume of 100 mL with sterilized DW and stored in an amber-colored bottle at 4°C for future use.

2.3. Biosynthesis of TiO_2-ZnO BNPs through the use of onion peel extract

The production of TiO_2-ZnO BNPs involved the use of distinct salt concentrations compared to traditional bimetallic biosynthesis protocols. Specifically, 10 ml of Zn $(NO_3)_2{\cdot}6H_2O$ and 10 ml of Ti $(NO_3)_4{\cdot}4H_2O$ (3.0 mM) were mixed and agitated for 25 min. Subsequently, 80 mL of the prepared onion peel extract was added to the metal salt solution. The pH of the final mixture was measured to be 8.0. To optimize the synthesis of TiO_2-ZnO BNPs for maximum profitability, the reaction conditions were meticulously adjusted. A shaking incubator set at 35°C was used to carry out the reaction with continuous agitation at 250 rpm for approximately 24 h [43]. Once the incubation period concluded, a color change to light reddish-brown was observed, suggesting the successful bioformation of TiO_2-ZnO BNPs. The nanoparticles were then washed five times with DW to eliminate any loosely bound organic compounds. Centrifugation was performed at 10,000 rpm for 10 min to ensure efficient purification of the synthesized BNPs.

2.4. TiO_2-ZnO BNP characterization

A visible color change in the onion peel extract, from red to pale reddish-brown, signified the onset of TiO_2-ZnO BNP synthesis. UV–visible spectroscopy was then used to measure the absorbance of the synthesized solution at wavelengths from 200 to 700 nm to determine the maximum surface plasmon resonance (SPR). FTIR analysis was conducted using the KBr pellet method in the wavenumber range of 400–4000 cm^{-1} to identify the chemical functional groups formed between the TiO_2-ZnO BNPs. TEM with a JEM-2100 Plus apparatus was deployed to determine the average dimensions and morphologies of the TiO_2-ZnO BNPs. DLS using a Nano ZS instrument from Malvern was implemented to measure the mean particle size distribution of the synthesized TiO_2-ZnO BNPs. XRD-6000, Shimadzu was harnessed to assess the crystal size and crystallinity of the bimetallic TiO_2-ZnO NPs. Together, these advanced characterization techniques offered comprehensive insights into the physicochemical and structural attributes of the green-synthesized TiO_2-ZnO BNPs.

2.5. Anti-microbial activity

2.5.1. Agar well method

A range of microbial strains were included as test specimens in the investigation, including *Bacillus subtilis* (ATCC 6633), *Staphylococcus aureus* (ATCC 6538), *Pseudomonas aeruginosa* (ATCC 9027), *Escherichia coli* (ATCC 25922), and *Candida albicans* (ATCC 10231). Pure cultures of microorganisms were subcultured using nutrient broth. The studied microorganisms were evenly distributed on sterilized petri dishes spread using Muller-Hinton agar. A 6 mm diameter well has been created in each plate employing a sterile cork-borer. A 100-μL aliquot of titanium and zinc oxide mixture, and TiO_2-ZnO BNPs were introduced to the well in order to assess the antimicrobial test. The plates were then incubated at 37°C and 30°C for 24 and 72 h, respectively, and the zones of inhibition were assessed. Each test was run three times [44]. MIC of TiO_2-ZnO BNPs was examined for several microbial strains at dosages ranging from 1000 μg mL^{-1} to 15.75 μg, using the broth microdilution method [45].

2.6. Biofilm inhibition assay

Using *S. aureus* (MRSA), a clinical isolate that was known to be an excellent biofilm producer, the MTP technique was utilized to examine the potential of TiO_2-ZnO BNPs to inhibit or diminish the biofilm development of bacteria. The biofilm experiment was conducted with slight modifications from the method described by Wahman et al. [46].

2.7. Anticancer activity

2.7.1. Cell viability assay

The MCF-7 and HepG2cancer cell lines used in this study were purchased from ATCC (Manassas, USA). To determine the cytotoxic capacity, the MTT method was used [47]. After being sown in 96-well plates at a density of 1.2 × 104 cells per well, the cells were given 24 h to grow. The medium containing the various nanoparticle concentrations was then refilled. After 48 h, 100 μL of a solution containing 5 mg/mL of MTT in PBS was blended to perform the MTT test. We next incubated the wells for 4 h at 37°C. Each well received 100 μL of DMSO to solve the formazan crystals. The incubation period for the plates was ten minutes at 37°C. Measurements taken at 570 nm with a Microplate reader (Epoc-2 C microplate reader, BioTek, USA) have been used to determine optical densities.

2.7.2. Assessment of caspase-8 activities

ELISA kits from DRG International Inc. (USA) investigated caspase-8 (human, EIA-4863).

2.7.3. VEGFR-2 TK inhibition assay performed in vitro using cell-based methods

Bimetallic titanium dioxide–zinc oxide (TiO_2-ZnO BNPs) was evaluated for the inhibition of VEGFR-2 using ten-fold dilutions (1.0, 0.1, 0.01, 0.001 μM). We utilized the VEGFR-2 (KDR) Kinase Assay Kit, Catalogue #40325, adhering to the manufacturer's guidelines. The master mix was uniformly distributed throughout all wells with a 25 μl aliquot. Introduce 5 μl of the inhibitor solution into the 'Test Inhibitor' well. In the 'Positive Control' and 'Blank' wells, 5 μl of solution devoid of inhibitors was introduced. A 3 ml kinase buffer was prepared by combining 600 μl with 2400 μl of distilled water. Subsequently, 20 μl of the buffer was dispensed into the 'Blank' wells. The VEGFR-2 enzyme was diluted to 1 ng/μl using kinase buffer to achieve the best working concentration. The reaction commenced with the addition of 20 μL of diluted enzyme to the 'Positive Control' and 'Test Inhibitor' wells. The reaction mixtures were incubated for 45 min at 30°C. Following the addition of 50 μl of Kinase-Glo Max reagent to each well, the plate was incubated at ambient temperature for 15 min. The light intensity was quantified using a microplate reader following incubation.

3. Statistical analysis

The collected data were subjected to statistical analysis using SPSS version 21 (SPSS Inc., Chicago, IL, USA). To compare multiple samples, an analysis of variance (ANOVA) was initially performed, followed by Tukey's post-hoc test. A p-value of less than 0.05 was considered statistically significant.

4. Results and discussion

4.1. Role of onion peel phytochemicals in BNP synthesis

The use of onion peel extract in the current study offers a novel and eco-friendly route for synthesizing TiO_2-ZnO BNPs [48]. Onion peels, often discarded as waste, are in fact rich in a variety of phytochemicals (including flavonoids, terpenoids, aldehydes, and carboxylic acids) which act as natural reducing and capping agents. These compounds facilitate the bioreduction of metal ions and stabilize the nanoparticles, preventing agglomeration and enhancing colloidal stability [49,50]. The color change to a pale reddish-brown observed during synthesis served as an initial visual indicator of nanoparticle formation, confirming the involvement of phytochemicals in the redox process. Flavonoids, in particular, play a key role through tautomeric transformations between enol and keto forms, releasing reactive hydrogen atoms that reduce the metal precursors to nanoscale particles [51,52]. Eco-friendly TiO_2 nanoparticles were synthesized and characterized by Ali et al. [53] incorporating both onion and garlic peel extracts.

Several studies have highlighted the effectiveness of biological sources in synthesizing metal and bimetallic nanoparticles for diverse applications. For instance, Khamis et al. [54] successfully synthesized ZnO using red onion extract, which demonstrated potential in antibacterial activity and dye degradation. In a separate study, the fungal strain *Aspergillus niger* AH1 facilitated the biosynthesis of ZnO-CuO nanocomposites supported on carbon scaffolds (ZnO-CuONPs/CSC) through its metabolic products [55]. Hashem and El-Sayyad [19] prepared synthesized bimetallic Ag-ZnO nanoparticles using pomegranate peel extract (PPE). Zinc and silver nitrates decreased, causing the solution color to change from translucent to light brown. PPE acted as both a reducing and stabilizing agent, resulting in the formation of stable colloidal nanoparticles. Furthermore, Fouda et al. [56] used *Ulva fasciata* Delile, a marine macroalga, to phyco-synthesize ZnO nanoparticles with demonstrated applications in antimicrobial activity, photocatalysis, and treatment of tanning industry wastewater. Khalil et al. [57] utilized *Pluchea indica* leaf extract to produce selenium-gold bimetallic nanoparticles and explored their potential biological effects. Similarly, Hashem et al. [58] used watermelon rind as a reducing agent in the biosynthesis of selenium-silver bimetallic nanoparticles. In another related work, Hashem et al. [59] synthesized ZnO@SeO bimetallic nanoparticles using PPE, revealing promising antibacterial, antifungal, and anticancer activities. This represents a clear advancement, as bimetallic systems often exhibit enhanced biological activity due to synergistic effects between the two metal oxides. Moreover, the successful synthesis using onion peel highlights the valorization of agro-waste, turning an abundant and low-cost byproduct into a powerful nanomaterial precursor [37]. This approach not only aligns with sustainable nanotechnology goals but also provides a scalable and green alternative to chemical synthesis methods.

4.2. Characterization of the biosynthesized TiO_2-ZnO BNPs

The potential of onion peel extract to biosynthesize TiO_2-ZnO BNPs was clearly demonstrated through the color change observed during the synthesis process. Initially, the onion peel extract exhibited a red hue, which transitioned to a pale red-brown color upon reaction with zinc nitrate and titanium nitrate. This color shift is indicative of the activation of SPR, a phenomenon that occurs due to the collective oscillation of conduction electrons on the nanoparticle surface [49]. The UV–Vis spectroscopy results confirmed the formation of the TiO_2-ZnO BNPs, with a peak observed at approximately 320.0 nm (Fig. 1). The optical density of 1.044, observed after a twofold dilution, further supports the presence of nanoparticles in the solution, consistent with prior studies in the literature [53,60]. The peak in the UV–Vis spectrum of the synthesized nanoparticles aligns with typical SPR peaks observed for TiO_2-ZnO BNPs, confirming their successful biogenesis.

The UV–Vis spectrum of the synthesized TiO_2-ZnO BNPs closely resembles those of previous studies, such as the biosynthesis of

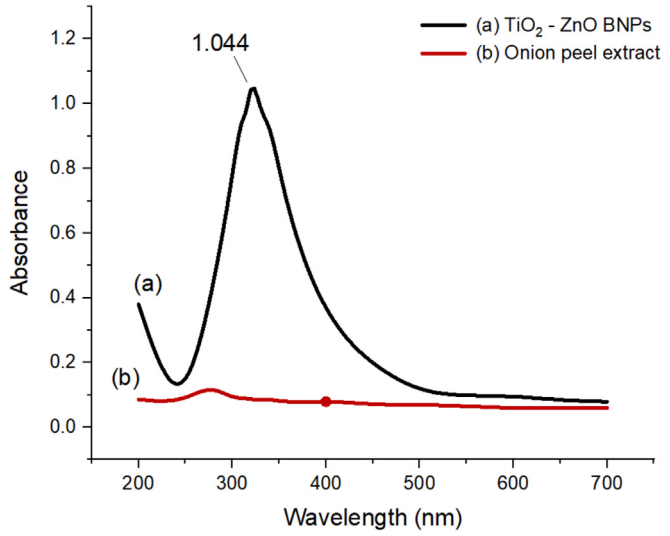

Fig. 1. (a) UV–Vis spectrum of TiO_2-ZnO BNPs synthesized using onion peel extract. (b) UV–Vis spectrum of onion peel extract.

ZnO-CuO NPs, where peaks at 326, 365, and 410 nm were indicative of metal oxide heterojunctions [55]. In contrast, the absence of multiple peaks in our spectrum suggests a more uniform nanoparticle formation without significant heterojunction features. This uniformity is likely due to the plant extract's bioactive phytochemicals, which play a dual role as reducing agents and capping agents to prevent nanoparticle agglomeration [50]. Additionally, the phytochemicals found in onion peel, such as flavonoids and terpenoids, are known to facilitate the reduction of metal ions and stabilize nanoparticles by preventing their aggregation [51,52]. These compounds interact with metal ions, undergoing tautomeric reactions that release reactive hydrogen atoms, which in turn reduce the metal ions into nanoparticles [51]. This process is particularly efficient for the production of bimetallic nanoparticles, as demonstrated by the successful synthesis of TiO_2-ZnO BNPs in this study. In a different investigation, the bimetallic B_2O_3-ZnO NP solution was transformed into a deep off-white color. The produced B_2O_3-ZnO NPs were small and detectable at 370.0 nm, according to the UV–Vis studies [61]. Due to the O.D. 0.295, Hashem et al. [58] noticed the UV–visible spectrum, which was located at 380 nm. The color change observed during the synthesis, coupled with the SPR peak at 320 nm, indicates a strong interaction between the TiO_2 and ZnO domains in the bimetallic nanoparticles. These interactions may enhance their photocatalytic, antimicrobial, and anticancer activities, as has been shown in other studies involving similar biosynthesized nanoparticles [55,58].

4.2.1. Morphology and size by TEM

The TEM revealed that the biosynthesized TiO_2-ZnO BNPs exhibited a monodisperse distribution with well-defined pentagonal morphologies. The particle sizes ranged between 80 and 170 nm (Fig. 2a), indicating a relatively uniform shape and size, which reflects the effectiveness of the onion peel extract in

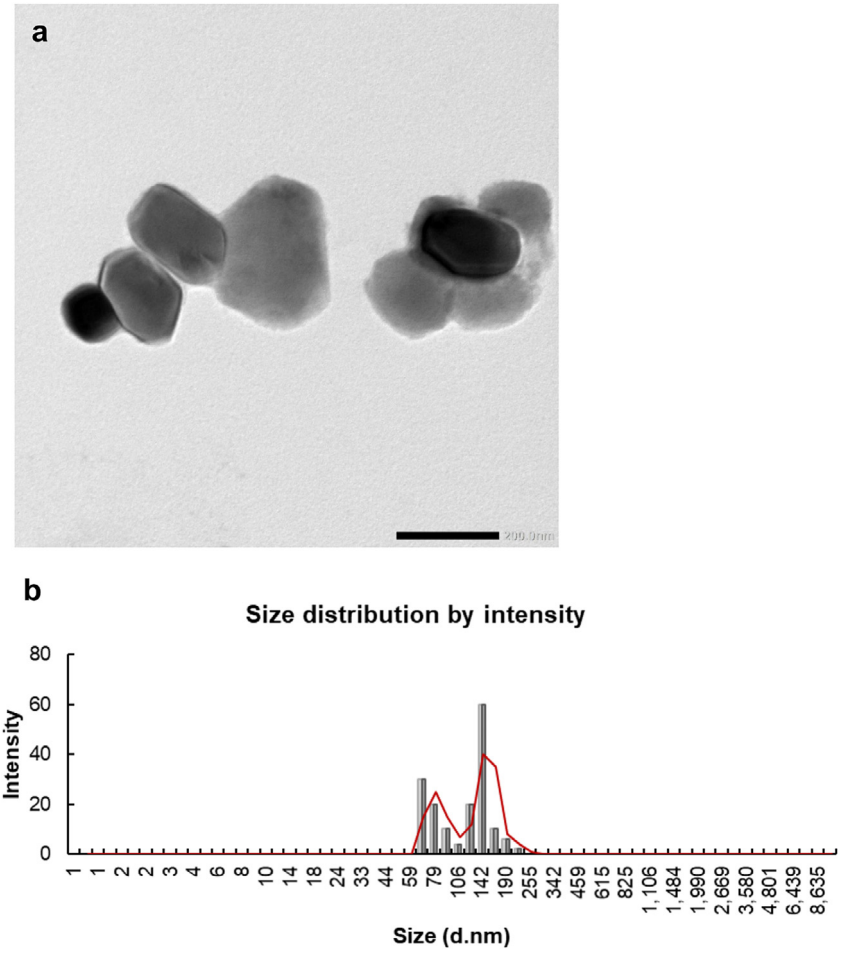

Fig. 2. TEM (a) and DLS (b) images of TiO_2-ZnO BNPs showing pentagonal morphology and size distribution.

controlling nanoparticle growth and stability. The presence of pentagonal structures is particularly notable, as it reflects a level of structural regularity that may be associated with enhanced surface energy minimization during the nucleation process. This pentagonal geometry is relatively uncommon but has been reported in certain biosynthesized nanostructures where plant extracts play a templating role. Previous findings by Hashem et al. [58] demonstrated biosynthesized Se-Ag nanoparticles within a smaller size range (18.3–49.6 nm), exhibiting different morphological characteristics. Similarly, Elkady et al. [62] observed spherical and oval morphologies in St/Ag-Se nanocomposites, with a mean size of 67.87 nm. Lee et al. [63] successfully synthesized Au–Ag BNPs with an average size of 80.4 ± 11.9 nm by using Korean red ginseng (*Panax ginseng Meyer*) root extract. Elsayed et al. [64] fabricated ZnO–Ag bimetallic nanoparticles with a size distribution between 30 and 130 nm. Their study further confirmed the successful formation of the bimetallic nanocomposite using multiple characterization techniques. These differences in size and shape can largely be attributed to the nature of the biological reducing agents and synthesis conditions employed [49]. Additionally, the formation of pentagonal-shaped nanoparticles suggests a unique nucleation and growth pathway, possibly influenced by specific flavonoids, phenolics, or sulfur-containing compounds abundant in the extract.

4.2.2. Hydrodynamic size by DLS and PDI implications

The dynamic light scattering technique further characterized the hydrodynamic diameter of the TiO_2-ZnO BNPs, revealing a broader size distribution between 60 and 190 nm, with predominant average sizes at 70 and 142 nm (Fig. 2b). These values were slightly larger than those obtained through TEM, which is expected due to the presence of a hydration shell surrounding the particles in colloidal suspension a factor that DLS captures, unlike TEM which observes dry particles [65]. The measured polydispersity index (PDI) was 0.332, falling within the accepted range (<0.7), indicative of a moderate but acceptable level of monodispersity [66]. A lower PDI signifies that the synthesized nanoparticles have consistent sizes and exhibit stable colloidal behavior, which is critical for applications where uniformity affects functionality such as catalysis, drug delivery, or photocatalysis. The typical particle size distribution of the bimetallic AgZnO NPs biosynthesized by the generated PPE was found to be 21.20 nm by the DLS technique, according to the work of Hashem and El-Sayyad [19]. Hashem et al. [61] determined that the particle size distribution of bimetallic B_2O_3-ZnO NPs, synthesized utilizing Gum Arabic and gamma rays, averaged 70.54 nm.

4.2.3. FTIR characterization of onion peel extract and TiO_2-ZnO BNPs

This study used FTIR spectroscopy to analyze the functional groups in onion peel extract (B: FTIR spectrum of the onion peel extract) and to verify the production of TiO_2-ZnO BNPs (A: FTIR spectrum of TiO_2-ZnO BNPs).

The functional groups of TiO_2-ZnO BNPs were characterized using FT-IR research within the 400–4000 cm^{-1} spectrum. Fig. 3 displays the extracted spectra with peaks at 2163, 2037, 1977, 1606, and 1407 cm^{-1}, signifying stretching vibrations for alkyne (C≡C), carbonyl (C═O), and aromatic (C═C) molecules. Common phytochemicals in plant extracts are flavonoids, phenolic acids, and polyphenolic compounds [67,68]. In the spectra of TiO_2-ZnO BNPs, additional bands were seen at 3397 and 3047 cm^{-1}, corresponding to O—H and C—H stretching vibrations, respectively. The lack of these peaks in the pure extract signifies that certain bioactive compounds from the extract were adsorbed onto the nanoparticles' surface during production, aiding in capping and stability [69]. This observation is consistent with previous studies reporting the interaction of hydroxyl and aliphatic groups with the surface of metal and metal oxide nanoparticles synthesized using plant extracts [70,71]. Furthermore, characteristic absorption bands at 533 and 476 cm^{-1} in the BNP spectrum indicate the formation of Zn—O and Ti—O bonds, confirming the successful synthesis of bimetallic oxide nanoparticles [49,72]. These bands are generally considered fingerprints for metal–oxygen bonds in nanostructured materials. Overall, these results confirm that the onion peel extract served as both a reducing and stabilizing agent in the green synthesis of TiO_2-ZnO BNPs.

4.2.4. XRD analysis of TiO_2-ZnO BNPs

Fig. 4 displays the XRD patterns of biosynthesized TiO_2-ZnO BNPs, revealing both crystalline and partially amorphous characteristics. The observed diffraction peaks corresponding to TiO_2 are located at 2θ values of approximately 25.2°, 37.7°, 48.0°, 53.8°, 55.0°, and 62.6°, which are indexed to the (101), (004),

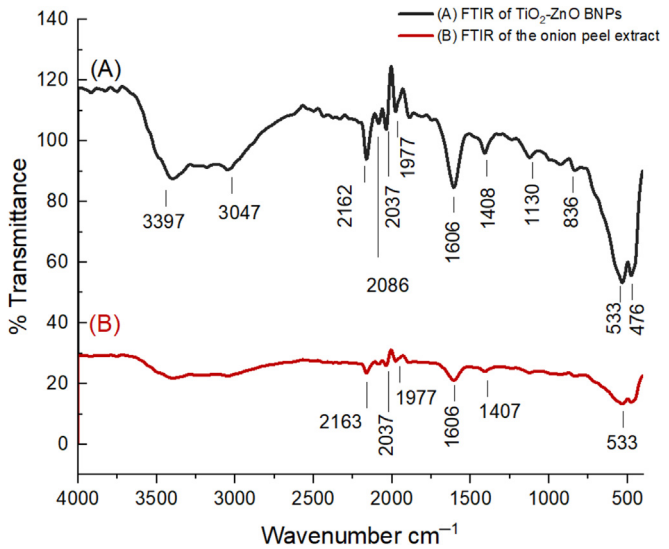

Fig. 3. A) FTIR of TiO_2-ZnO BNPs; and B) FTIR of the onion peel extract.

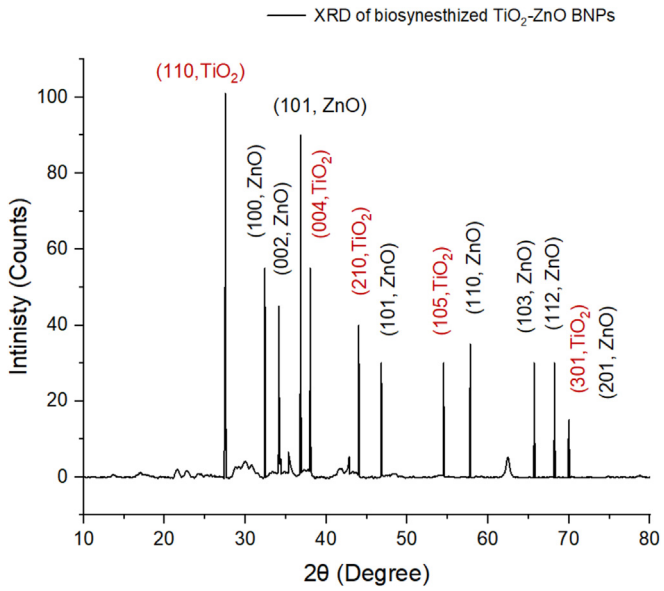

Fig. 4. XRD of biosynesthized TiO_2-ZnO BNPs synthesized using onion peel extract.

(200), (105), (211), and (204) planes of the anatase phase of TiO_2 (JCPDS card no. 21-1272) [73]. The corresponding D-spacing (hkl) values for TiO_2 are 3.53 Å, 2.37 Å, 1.89 Å, 1.68 Å, 1.66 Å, and 1.48 Å, respectively. Some additional minor peaks at 68.7°, 70.2°, 75°, and 76° may be attributed to minor phases, lattice strain, or instrumental factors [74]. Similar finding reported by Shekhar et al. [75] indicates that the (101), (004), (200), (105), and (204) planes are responsible for the reflection peaks found at 25°, 38°, 47°, 56°, and 61°, respectively. In addition, diffraction peaks attributed to ZnO NPs were observed at 2θ values of 31.7°, 34.4°, 36.2°, 47.5°, 56.6°, 62.8°, and 66.3°, corresponding to the (100), (002), (101), (102), (110), (103), and (200) planes, respectively, which are characteristic of the wurtzite hexagonal phase of ZnO (JCPDS card no. 36-1451) [76]. The corresponding D-spacing (hkl) values for ZnO are 2.81 Å, 2.59 Å, 2.47 Å, 1.91 Å, 1.63 Å, 1.47 Å, and 1.40 Å, respectively. Additional weak peaks at 68.1°, 69.2°, and 72.7° could be associated with interfacial effects, bimetallic interactions, or low-intensity crystalline reflections. Similar XRD profiles were also reported by Modi and Fulekar [77] and Masud et al. [78], who synthesized ZnO nanoparticles using garlic and Allium cepa peel extracts, respectively. These findings confirm the successful formation of highly crystalline TiO_2-ZnO BNPs with good phase purity. The average crystallite size was estimated using the Scherrer equation yielding a value of approximately 76 nm [79].

4.3. Antibacterial activity

The antimicrobial performance of the biosynthesized TiO_2-ZnO BNPs was evaluated against *E. coli, P. aeruginosa*, *B. subtilis, S. aureus,* and *C. albicans*. The inhibition zones for these pathogens were measured after treatment with TiO_2-ZnO BNPs at a concentration of 1000 μg/ml. The results revealed a significant antibacterial effect, with inhibition zones ranging from 11.4 to 13.8 mm, as displayed in Fig. 5. Reactive oxygen species-mediated as well as non-reactive species-mediated antimicrobial action have been the two likely ways that the TiO_2-ZnO NP composite demonstrates antibacterial properties [80]. According to Rashid et al. [81], whenever bacteria were exposed to biosynthesized ZnO NPs, they developed a heightened sensitivity to the antibacterial ciprofloxacin, whereas

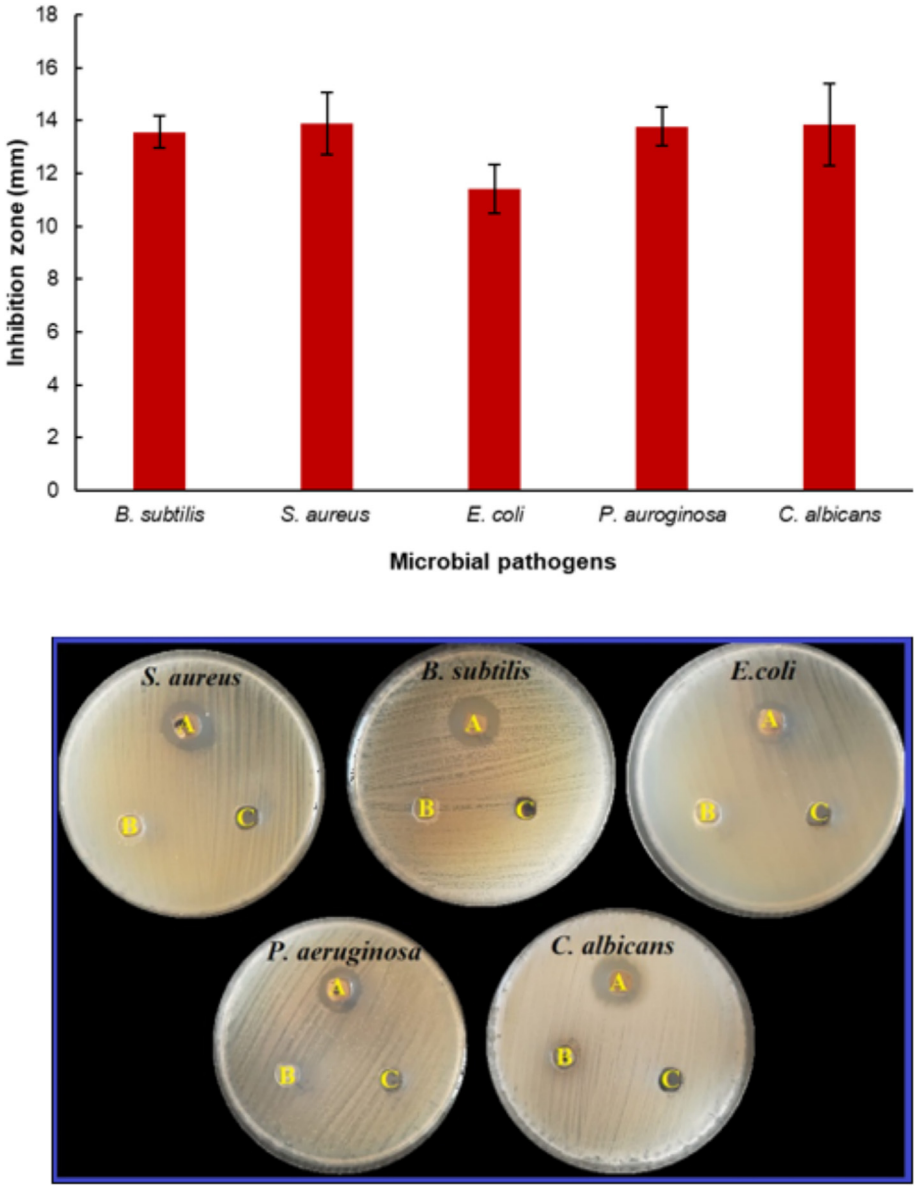

Fig. 5. Antimicrobial assay via Inhibition zones of TiO_2-ZnO BNPs using agar well method.

the antibiotic meropenem showed enhanced behavior. Additionally, it was noted that ZnO and TiO_2 NPs' antibacterial capability was dependent on time and developed gradually. The outcomes demonstrated that ZnO NPs outperformed TiO_2 in terms of efficiency [81]. Likewise, Rajashekara et al. [82] produced ZnO NPs by using leaf extract from *Calotropis gigantea* while discovering that it had potent antibacterial action towards each Gram-positive as well as negative bacteria. ZnO NPs produced impressive mean inhibition zone diameters (IZDs) for *P. aeruginosa, Klebsiella pneumoniae, E. coli, Salmonella enteritidis* and *Proteus mirabilis*, respectively, of 18 ± 1.02, 20 ± 1.04, 16 ± 0.08, 08 ± 0.82 and 22 ± 1.08 mm [83]. Nachimuthu et al. [84] reported that ZnO/Y_2O_3 NCs exhibited promising antibacterial activity toward *B. subtilis* and *S. aureus*. Elkady et al. [85] synthesized CuO-Se core-shell nanoparticles (50 nm) showing notable antibacterial activity against *P. aeruginosa*, with inhibition zones of 10–21 mm and 38–95 % growth reduction. MIC and MBC values ranged from 7.8–250 μg/mL to 31.2–500 μg/mL, with tolerance levels between 2 and 16.

4.3.1. Determination of MIC

The results showed that MIC of TiO_2-ZnO BNPs was 500 μg/mL for *B. subtilis, P. aeruginosa*, and *C. albicans*. For *S. aureus* and *E. coli*, the MIC values were 1000 μg/mL and 250 μg/mL, respectively (Fig. 6). TiO_2 NPs exhibited superior antibacterial efficacy compared to tetracycline, a commercially available antibiotic. This significantly reduces the probability of microorganisms acquiring resistance to these medications [86]. TiO_2 NPs at 100 μg/mL suppressed the growth of a variety of pathogenic bacteria and fungi [87]. Considering a wide range of species, ZnO-NPs may be proven to be an incredibly selective antibacterial agent that inhibits the growth of bacteria [88]. The remarkable antibacterial effectiveness of the green-synthesized Tb-ZnO-TiO_2NPs composite versus *K. pneumoniae, E. coli, Streptococcus mutans*, and *S. aureus* at dosages was shown by Shivalingam et al. [89], which the Tb-ZnO-TiO_2 NPs combination showed a wider zone of suppression in comparison to the antibiotic standard, suggesting a notably greater degree of activity against bacteria. As demonstrated in a previous study, TiO_2-Zno NPs had a MIC of about 10 μg/mL versus *S. aureus* (MRSA), and *Streptococcus pneumoniae* [90]. Agreeing with Pauzi et al. [91], ZnO nanoparticles ensured MIC of 31.25 μg mL^{-1} for *S. aureus* and 62.5 μg mL^{-1} for *E. coli*. Selim et al. [60] reported antimicrobial activity against *K. pneumoniae, E. coli, B. cereus, S. aureus*, and *C. albicans*, with MIC values between 31.25 and 250 μg/mL. Khalil et al. [57] demonstrated that Se–Au bimetallic nanoparticles exhibited antibacterial activity against *E. coli, P. aeruginosa, S. aureus*, and *B. subtilis*, with MICs of 31.25, 15.62, 31.25, and 3.9 μg/mL, respectively. Hasanin et al. [55] reported that the synthesized nanocomposite exhibited antibacterial effects against *B. subtilis, E. coli*, and *S. aureus* with MICs of 7.81, 31.25, and 62.5 μg/mL, respectively. It also showed antifungal activity against *Aspergillus brasiliensis* (MIC: 7.81 μg/mL), but limited efficacy against *Cryptococcus neoformans* and *C. albicans* (MIC: 250 μg/mL).

4.4. Antibiofilm activity

The formation of biofilms poses a significant challenge to antibacterial treatments as they provide bacteria with a greater resistance to traditional medicines [92]. TiO_2-ZnO BNP antibiofilm activity observed in this study exhibited a range of effects against MRSA. The TiO_2-ZnO BNP was therefore significantly inhibited action, with inhibition reaching 63.1% at 125 μg/mL and 24.7% at 7.8 μg/mL which was noticed to be the strongest inhibition of MRSA biofilm formation without hindering bacterial growth (Fig. 7). Earlier studies clarified the anti-biofilm action based on SEM pictures that revealed the presence of bacterial cell cracking, exterior cell hardness, and shrinking of the cell's inner wall. Additionally, less cellular viability and biofilm development were observed [93]. Considering this, Doğan and Kocabas [94] created ZnO NPs using *Veronica multifida* leaf extracts under varied physical situations. The produced NPs' antibiofilm activity was assessed versus *P. aeruginosa* as well as *S. aureus*. The findings showed that 50 μg/ml ZnO NPs at pH 12 reduced 87% of the biofilm formation in *S. aureus*, whereas 10 μg/ml ZnO NPs at pH 7 suppressed 88% of the biofilm formation. In *P. aeruginosa*, the highest dose of 50 μg/ml was shown to have the greatest biofilm inhibitory action at both pH 7 and pH 12 [94]. ZnO NPs, on the contrary hand, demonstrated 100 % better antibiofilm action towards *E. coli* [95]. TiO_2NPs produced from plants were evaluated and shown to exhibit antibacterial as well as antibiofilm properties on skin and intestinal infections, though at elevated levels in a relatively recently published study [96]. Additionally, it was shown that biofilm-forming microorganisms resistant to several drugs lost viability and that TiO_2 inhibited the production of biofilm depending on the concentration mode [97]. Moreover, Jin et al. [96] produced titanium dioxide nanoparticles using *Rosa davurica* leaf extract (RDL-TiO_2NPs) and assessed their antibiofilm efficacy against vari-

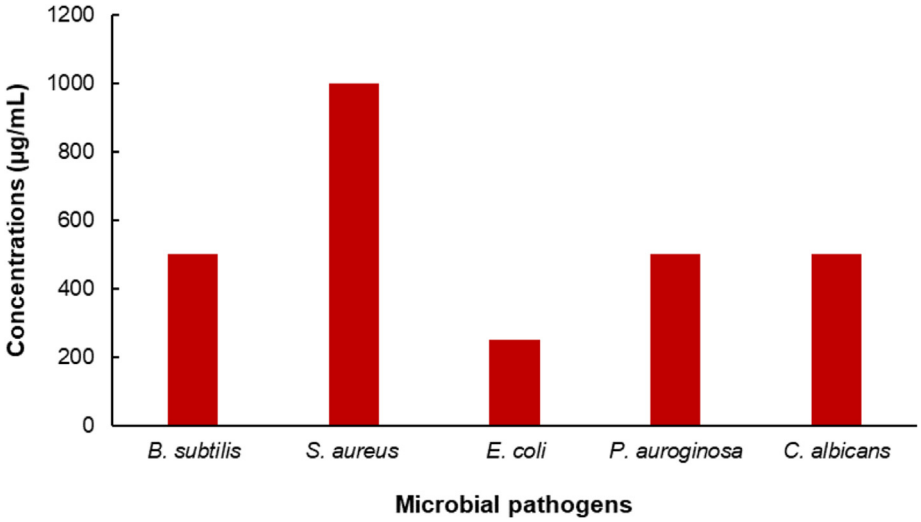

Fig. 6. MICs of TiO_2-ZnO BNPs toward tested bacterial and fungal strains.

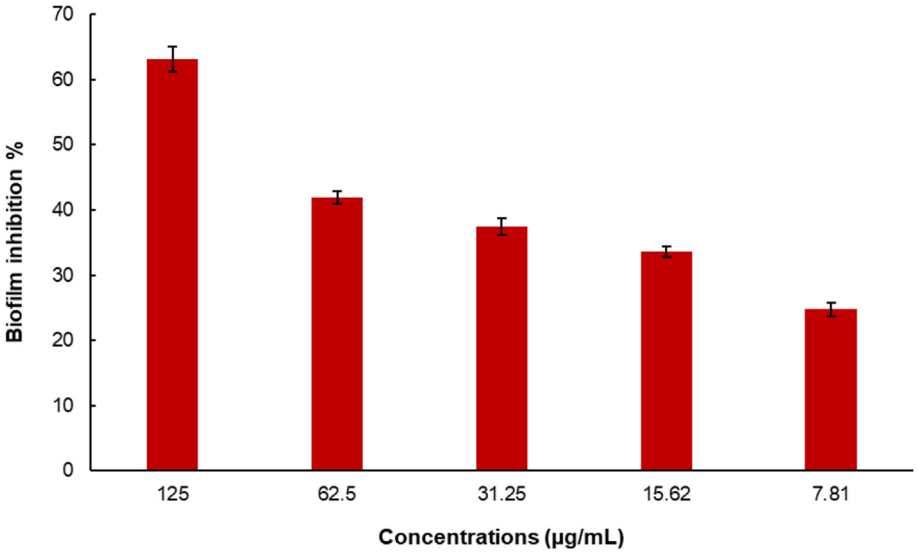

Fig. 7. Antibiofilm activity of TiO_2-ZnO BNPs.

ous bacteria that produce biofilms. Additionally, *S. aureus* and *S. enterica* had IC_{50} values of 76.84 and 158.75 µg/ml, correspondingly. RDL-TiONPs also inhibited bacterial biofilm by rupturing cell walls and membranes, according to the results of the TEM and CV assays [96]. Remarkably, Dan and Khan [98] investigated the antibiofilm properties of green produced titanium oxide towards *P. aeruginosa, E. coli, S. aureus*, and *C. albicans* by employing an extract from the leaves of *Ocimum sanctum*. According to their findings, these nanoparticles had an effective range of 250–650 µg/ml, with a lowest effective dosage of 450 µg/ml versus *E. coli*. For the other microorganisms, 250 µg/ml was enough [98]. Additionally, Elkady et al. [85] evaluated the antibiofilm activity of bimetallic copper oxide-selenium nanoparticles toward *P. aeruginosa* isolated where results illustrated that the maximum antibiofilm activity was 60.41% toward *P. aeruginosa* no. 5. Selim et al. [60] found that the MgO-ZnO nanocomposite exhibited antioxidant activity, with an IC_{50} of 175 µg/mL based on the DPPH assay.

4.5. *Cytotoxic effect of TiO_2-ZnO BNPs*

The cytotoxic activities of TiO_2-ZnO BNPs were assessed on HepG2 and MCF-7, respectively. The MCF-7 cells exhibited the most significant cytotoxic impact, as evidenced by their minimal IC_{50} values (Fig. 8).

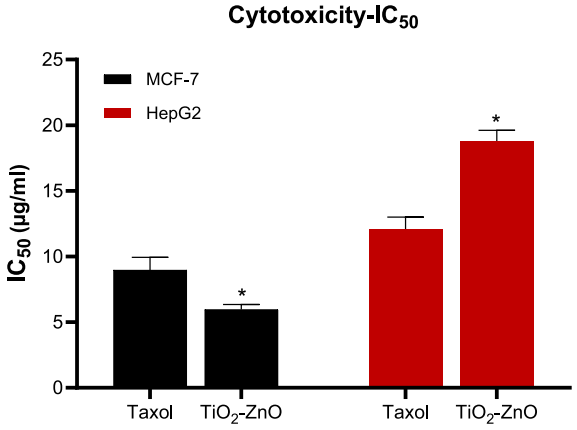

Fig. 8. *In vitro* cytotoxic activities of TiO_2-ZnO BNPs against MCF-7 and HepG2 cell lines.

TiO_2-ZnO BNPs resulted in a minimal IC_{50} value of 5.97 ± 0.37 µg/mL, while the IC_{50} for taxol was 8.96 ± 0.98 µg/mL. The MCF-7 cells are more vulnerable to the cytotoxic impacts of TiO_2-ZnO BNPs due to their increased expression of receptors and cell surface markers in breast cancer cells, which increases susceptibility. Conversely, HepG2 cells exhibit a greater antioxidant capacity than MCF-7 cells. This antioxidant defense can potentially reduce the cytotoxic activity of TiO_2-ZnO BNPs toward HepG2 cells, thereby mitigating their cytotoxic effects [99,100]. Hashem et al. [58] evaluated the cytotoxicity of Se-Ag BNP on the normal Wi38 cell line, reporting an IC_{50} value of 168.42 µg/mL, indicating acceptable biocompatibility.

4.5.1. *Effect of TiO_2-ZnO BNPs on caspase-8 activity*

TiO_2-ZnO BNP influences the apoptotic marker caspase-8 (Table 1). Exposure of MCF-7 cells to TiO_2-ZnO BNPs significantly increased caspase-8 activity (2.044 ± 0.06 ng/mL) in comparison to the control (0.341 ± 0.02 ng/mL). Furthermore, when exposed to TiO_2-ZnO BNPs, caspase-8 activity was markedly greater than with Taxol treatments (0.986 ± 0.03 ng/mL). Apoptosis triggers the activation of DNA fragmentation enzymes by activating caspase-8 [101]. These compounds induced apoptosis in MCF-7 cells by activating caspase-8.

4.6. *Effect of TiO_2-ZnO BNPs on VEGFR-2 activity*

The inhibition concentration–response curve was utilized to determine the 50 % inhibition concentration value (IC_{50}) (Fig. 9). Sorafenib served as the positive control in this test. The TiO_2-ZnO BNPs exhibited significant inhibitory activity, with an IC_{50} value of 0.241 ± 0.009 µg/ml. VEGF expression is elevated in breast cancer cells relative to normal tissues. The reduced expression of the

Table 1
Effect of TiO_2-ZnO BNPs on caspase-8 (ng/mL) in MCF-7 cells.

Comp. ID	Caspase-8 (ng/mL)
	MCF-7
Control	0.341 ± 0.02
Taxol	0.986 ± 0.03
TiO_2-ZnO BNPs	2.044 ± 0.06

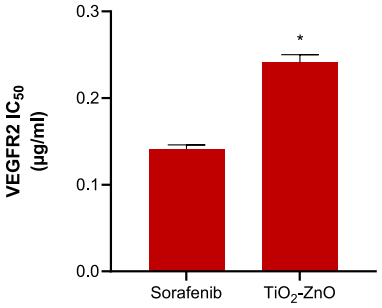

Fig. 9. Effects of TiO_2-ZnO BNPs on VEGFR-2 in MCF-7 cells.

VEGF receptor (VEGFR-2) indicates an anti-angiogenic impact. VEGF is a powerful angiogenic factor that stimulates tumor development and angiogenesis in breast cancer. However, a reduction in VEGFR-2 expression hampers the capacity of VEGF to promote angiogenesis. The simultaneous decrease in VEGFR expression might result in a decline in the formation of new blood vessels, which can be advantageous in cancer therapy, where excessive blood vessel formation can promote tumor development and spread [102,103].

5. Conclusions

In conclusion, the innovative approach of synthesizing bimetallic titanium dioxide-zinc oxide (TiO_2-ZnO) nanoparticles using onion peel extract not only addresses the pressing issues of antibiotic resistance and cancer treatment but also exemplifies the power of sustainable methods in nanotechnology. The successful characterization of these nanoparticles, alongside their effective antimicrobial and anticancer properties, underscores their potential as multifunctional therapeutic agents. This research paves the way for further exploration of plant-based materials in the development of nanomaterials, showcasing a promising avenue for future biomedical applications.

Moreover, the significant antimicrobial and cytotoxic effects demonstrated by the TiO_2-ZnO BNPs suggest their applicability in clinical settings, particularly for patients suffering from resistant infections and cancer. The dual functionality of these nanoparticles may lead to more effective treatment strategies, potentially reducing the reliance on traditional antibiotics and enhancing cancer therapies. As the demand for eco-friendly and efficient solutions in medicine grows, this study highlights the importance of harnessing natural resources in the synthesis of nanomaterials, offering hope for innovative treatments in the fight against major health challenges.

CRediT authorship contribution statement

Ebrahim Saied: Writing – original draft, Conceptualization, Writing – review & editing. **Ahmed S. Doghish:** Data curation, Resources. **Mohamed K.Y. Soliman:** Conceptualization, Validation. **Walaa A. El-Dakroury:** Formal analysis, Methodology. **Abeer S. Aloufi:** Conceptualization, Funding acquisition. **Bushra Hafeez Kiani:** Resources, Software. **Amr H. Hashem:** Writing – review & editing, Conceptualization, Writing – original draft.

Financial support

Princess Nourah bint Abdulrahman University Researchers Supporting Project number (PNURSP2025R357), Princess Nourah bint Abdulrahman University, Riyadh, Saudi Arabia.

Declaration of competing interest

The authors declare that they have no known competing financial interests or personal relationships that could have appeared to influence the work reported in this paper.

Supplementary material

https://doi.org/10.1016/j.ejbt.2025.06.001.

Data availability

Data will be made available on request.

References

[1] Haleem A, Javaid M, Singh RP, et al. Applications of nanotechnology in medical field: A brief review. Glob Health J 2023;7(2):70–7. https://doi.org/10.1016/j.glohj.2023.02.008.
[2] Samuel MS, Ravikumar M, John JA, et al. A review on green synthesis of nanoparticles and their diverse biomedical and environmental applications. Catalysts 2022;12(5):459. https://doi.org/10.3390/catal12050459.
[3] Hheidari A, Mohammadi J, Ghodousi M, et al. Metal-based nanoparticle in cancer treatment: Lessons learned and challenges. Front Bioeng Biotechnol 2024;12:1436297. https://doi.org/10.3389/fbioe.2024.1436297. PMid: 39055339.
[4] Chandrakala V, Aruna V, Angajala G. Review on metal nanoparticles as nanocarriers: Current challenges and perspectives in drug delivery systems. Emerg Mater 2022;5:1593–615. https://doi.org/10.1007/s42247-021-00335-x. PMid: 35005431.
[5] Soliman MK, Abu-Elghait M, Salem SS, et al. Multifunctional properties of silver and gold nanoparticles synthesis by *Fusarium pseudonygamai*. Biomass Convers Biorefin 2024;14:28253–70. https://doi.org/10.1007/s13399-022-03507-9.
[6] Idris DS, Roy A. Synthesis of bimetallic nanoparticles and applications—An updated review. Crystals 2023;13(4):637. https://doi.org/10.3390/cryst13040637.
[7] Sajid M. Nanomaterials: Types, properties, recent advances, and toxicity concerns. Curr Opin Environ Sci Health 2022;25:100319. https://doi.org/10.1016/j.coesh.2021.100319.
[8] Joudeh N, Linke D. Nanoparticle classification, physicochemical properties, characterization, and applications: A comprehensive review for biologists. J Nanobiotechnol 2022;20:262. https://doi.org/10.1186/s12951-022-01477-8. PMid: 35672712.
[9] Liu L, Corma A. Bimetallic sites for catalysis: From binuclear metal sites to bimetallic nanoclusters and nanoparticles. Chem Rev 2023;123(8):4855–933. https://doi.org/10.1021/acs.chemrev.2c00733. PMid: 36971499.
[10] Almuhayawi MS, Alruhaili MH, Soliman MK, et al. Investigating the *in vitro* antibacterial, antibiofilm, antioxidant, anticancer and antiviral activities of zinc oxide nanoparticles biofabricated from *Cassia javanica*. PLoS One 2024;19(10):e0310927. https://doi.org/10.1371/journal.pone.0310927. PMid: 39352889.
[11] Ventola CL. The antibiotic resistance crisis: Part 1: Causes and threats. Pharm Ther 2015;40(4):277–83. PMid: 25859123.
[12] Selim MT, Soliman MK, Hashem AH. Biosynthesis of silver nanoparticles from endophytic fungi and their role in plant disease management. In: Abd-Elsalam KA, Hashem AH, editors. Fungal endophytes volume II: Applications in agroecosystems and plant protection. Singapore: Springer Nature Singapore; 2025. p. 357–82. https://doi.org/10.1007/978-981-97-8804-0_12.
[13] Soliman MK, Amin MA-A, Nowwar AI, et al. Green synthesis of selenium nanoparticles from *Cassia javanica* flowers extract and their medical and agricultural applications. Sci Rep 2024;14:26775. https://doi.org/10.1038/s41598-024-77353-2. PMid: 39500933.
[14] Nwobodo DC, Ugwu MC, Anie CO, et al. Antibiotic resistance: The challenges and some emerging strategies for tackling a global menace. J Clin Lab Anal 2022;36(9):e24655. https://doi.org/10.1002/jcla.24655. PMid: 35949048.
[15] Muruganandham M, Al-Otibi FO, Alharbi RI, et al. Antibacterial, antifungal, antioxidant, and cytotoxicity activities of the aqueous extract of *Syzygium aromaticum*-mediated synthesized novel silver nanoparticles. Green Process Synth 2023;12(1):20230188. https://doi.org/10.1515/gps-2023-0188.
[16] Brianna Lee SH. Chemotherapy: How to reduce its adverse effects while maintaining the potency? Med Oncol 2023;40:88. https://doi.org/10.1007/s12032-023-01954-6. PMid: 36735206.
[17] Shehabeldine AM, Doghish AS, El-Dakroury WA, et al. Antimicrobial, antibiofilm, and anticancer activities of syzygium aromaticum essential oil nanoemulsion. Molecules 2023;28:5812. https://doi.org/10.3390/molecules28155812. PMid: 37570781.
[18] Ali OM, Hasanin MS, Suleiman WB, et al. Green biosynthesis of titanium dioxide quantum dots using watermelon peel waste: Antimicrobial,

antioxidant, and anticancer activities. Biomass Convers Biorefin 2024;14:6987–98. https://doi.org/10.1007/s13399-022-02772-y.
[19] Hashem AH, El-Sayyad GS. Antimicrobial and anticancer activities of biosynthesized bimetallic silver-zinc oxide nanoparticles (Ag-ZnO NPs) using pomegranate peel extract. Biomass Convers Biorefin 2024;14:20345–57. https://doi.org/10.1007/s13399-023-04126-8.
[20] Hashem AH, Saied E, Ali OM, et al. Pomegranate peel extract stabilized selenium nanoparticles synthesis: Promising antimicrobial potential, antioxidant activity, biocompatibility, and hemocompatibility. Appl Biochem Biotechnol 2023;195:5753–76. https://doi.org/10.1007/s12010-023-04326-y. PMid: 36705842.
[21] Hashem AH, Selim TA, Alruhaili MH, et al. Unveiling antimicrobial and insecticidal activities of biosynthesized selenium nanoparticles using prickly pear peel waste. J Funct Biomater 2022;13(3):112. https://doi.org/10.3390/jfb13030112. PMid: 35997450.
[22] Salem SS, Badawy MSEM, Al-Askar AA, et al. Green biosynthesis of selenium nanoparticles using orange peel waste: Characterization, antibacterial and antibiofilm activities against multidrug-resistant bacteria. Life 2022;12(6):893. https://doi.org/10.3390/life12060893. PMid: 35743924.
[23] Sarathi R, Sheeba N, Essaki ES, et al. Titanium doped Zinc Oxide nanoparticles: A study of structural and optical properties for photocatalytic applications. Mater Today Proc 2022;64:1859–63. https://doi.org/10.1016/j.matpr.2022.06.387.
[24] Rahman KH, Kar AK. Titanium-di-oxide (TiO_2) concentration-dependent optical and morphological properties of PAni-TiO_2 nanocomposite. Mater Sci Semicond Process 2020;105:104745. https://doi.org/10.1016/j.mssp.2019.104745.
[25] Parrino F, Pomilla FR, Camera-Roda G. Properties of titanium dioxide. In: Parrino F, Palmisano L, editors. Titanium dioxide (TiO_2) and its applications. Elsevier; 2021. p. 13–66. https://doi.org/10.1016/B978-0-12-819960-2.00001-8.
[26] Smith R, Silwana B, Matoetoe MC. Electrochemical properties modulation of Zinc oxide nanoparticles. J Indian Chem Soc 2023;100(8):101054. https://doi.org/10.1016/j.jics.2023.101054.
[27] Nagaraj B, Malakar B, Divya T, et al. Synthesis of plant mediated gold nanoparticles using flower extracts of *Carthamus tinctorius* L. (Safflower) and evaluation of their biological activities. Dig J Nanomater Biostruct 2012;7(3):1289–95.
[28] Padmanabhan L, Divya T, Malakar B, et al. Preparation of gold nanoparticles from *Helianthus annuus* (sun flower) flowers and evaluation of their antimicrobial activities. Int J Pharm Bio Sci 2012;3(1):439–46.
[29] Lava MB, Muddapur UM, Basavegowda N, et al. Characterization, anticancer, antibacterial, anti-diabetic and anti-inflammatory activities of green synthesized silver nanoparticles using *Justica wynaadensis* leaves extract. Mater Today Proc 2021;46:5942–7. https://doi.org/10.1016/j.matpr.2020.10.048.
[30] Basavegowda N, Somu P, Shabbirahmed AM, et al. Bimetallic p-ZnO/n-CuO nanocomposite synthesized using *Aegle marmelos* leaf extract exhibits excellent visible-light-driven photocatalytic removal of 4-nitroaniline and methyl orange. Photochem Photobiol Sci 2022;21:1357–70. https://doi.org/10.1007/s43630-022-00224-0. PMid: 35451802.
[31] Mishra K, Basavegowda N, Lee YR. Biosynthesis of Fe, Pd, and Fe–Pd bimetallic nanoparticles and their application as recyclable catalysts for [3 + 2] cycloaddition reaction: A comparative approach. Cat Sci Technol 2015;5:2612–21. https://doi.org/10.1039/C5CY00099H.
[32] Abu-Elghait M, Soliman MK, Azab MS, et al. Response surface methodology: Optimization of myco-synthesized gold and silver nanoparticles by *Trichoderma saturnisporum*. Biomass Convers Biorefin 2025;15:4211–24. https://doi.org/10.1007/s13399-023-05188-4.
[33] Ahmed SF, Mofijur M, Rafa N, et al. Green approaches in synthesising nanomaterials for environmental nanobioremediation: Technological advancements, applications, benefits and challenges. Environ Res 2022;204(Part A):111967. https://doi.org/10.1016/j.envres.2021.111967.
[34] Zhou F, Peterson T, Fan Z, et al. The commonly used stabilizers for phytochemical-based nanoparticles: Stabilization effects, mechanisms, and applications. Nutrients 2023;15(18):3881. https://doi.org/10.3390/nu15183881. PMid: 37764665.
[35] Kang C-W, Kolya H. Green synthesis of Ag-Au bimetallic nanocomposites using waste tea leaves extract for degradation Congo red and 4-nitrophenol. Sustainability 2021;13(6):3318. https://doi.org/10.3390/su13063318.
[36] Sonu, Rani GM, Pathania D, et al. Agro-waste to sustainable energy: A green strategy of converting agricultural waste to nano-enabled energy applications. Sci Total Environ 2023;875:162667. https://doi.org/10.1016/j.scitotenv.2023.162667. PMid: 36894105.
[37] Kaur N. An innovative outlook on utilization of agro waste in fabrication of functional nanoparticles for industrial and biological applications: A review. Talanta 2024;267:125114. https://doi.org/10.1016/j.talanta.2023.125114. PMid: 37683321.
[38] Suliman AA, El-Dewiny CY, Soliman MK, et al. Investigation of the effects of applying bio-magnesium oxide nanoparticle fertilizer to *Moringa oleifera* plants on the chemical and vegetative properties of the plants' leaves. Biotechnol J 2025;20(3):e202400536. https://doi.org/10.1002/biot.202400536. PMid: 40059570.
[39] Brar KK, Magdouli S, Othmani A, et al. Green route for recycling of low-cost waste resources for the biosynthesis of nanoparticles (NPs) and nanomaterials (NMs)-A review. Environ Res 2022;207:112202. https://doi.org/10.1016/j.envres.2021.112202. PMid: 34655607.
[40] Rodrigues AS, Almeida DP, Simal-Gándara J. Onions: A source of flavonoids. In: Justino GC, editor. Flavonoids: From biosynthesis human health. InTech; 2017. p. 439. https://doi.org/10.5772/intechopen.69896.
[41] Lohri CR, Diener S, Zabaleta I, et al. Treatment technologies for urban solid biowaste to create value products: A review with focus on low-and middle-income settings. Rev Environ Sci Bio/Technol 2017;16:81–130. https://doi.org/10.1007/s11157-017-9422-5.
[42] Jasim NO, Abd-Ali NK. Biosynthesis of ZnO nanoparticle in presence of red onion extract. Plant Arch 2020;20(2):7854–6.
[43] Muhammad NAM, Awang NA, Mahmud NNHEN, et al. Biosynthesized zinc oxide and titanium dioxide nanoparticles by aloe vera extract for tunable Q-switched application. Opt Fiber Technol 2023;77:103276. https://doi.org/10.1016/j.yofte.2023.103276.
[44] Perez C, Pauli M, Bazerque P. An antibiotic assay by agar-well diffusion method. Acta Biologiae et Medicinae Exp 1990;15:113–5.
[45] Abbey TC, Deak E. What's new from the CLSI subcommittee on antimicrobial susceptibility testing M100. Clin Microbiol Newsl 2019;41(23):203–9. https://doi.org/10.1016/j.clinmicnews.2019.11.002.
[46] Wahman S, Emara M, Shawky RM. *In-vitro* assessment of staphylococci biofilms formed under biologically-relevant conditions and correlation to the biofilm genotype. Res J Pharm Technol 2023;16(5):2273–9. https://doi.org/10.52711/0974-360X.2023.00373.
[47] Mosmann T. Rapid colorimetric assay for cellular growth and survival: Application to proliferation and cytotoxicity assays. J Immunol Methods 1983;65(1–2):55–63. https://doi.org/10.1016/0022-1759(83)90303-4. PMid: 6606682.
[48] Toppo SR. Nanomaterials' synthesis from the fruit wastes. In: Bhardwaj AK, Srivastav AR, Dwivedi K, editors. Green and sustainable approaches using wastes for the production of multifunctional nanomaterials. Elsevier; 2024. p. 345–64. https://doi.org/10.1016/B978-0-443-19183-1.00018-0.
[49] Dubey S, Virmani T, Yadav SK, et al. Breaking barriers in eco-friendly synthesis of plant-mediated metal/metal oxide/bimetallic nanoparticles: Antibacterial, anticancer, mechanism elucidation, and versatile utilizations. J Nanomater 2024;2024(1):9914079. https://doi.org/10.1155/2024/9914079.
[50] Ettadili FE, Aghris S, Laghrib F, et al. Recent advances in the nanoparticles synthesis using plant extract: Applications and future recommendations. J Mol Struct 2022;1248:131538. https://doi.org/10.1016/j.molstruc.2021.131538.
[51] Acharya C, Mishra S, Chaurasia SK, et al. Synthesis of metallic nanoparticles using biometabolites: Mechanisms and applications. Biometals 2025;38:21–54. https://doi.org/10.1007/s10534-024-00642-w. PMid: 39377881.
[52] Suhag R, Rohit K, Atul D, et al. Fruit peel bioactives, valorisation into nanoparticles and potential applications: A review. Crit Rev Food Sci Nutr 2023;63:6757–76. https://doi.org/10.1080/10408398.2022.2043237. PMid: 35196934.
[53] Ali H, Dixit S, Almutairi BO, et al. Synthesis and characterization of eco-friendly TiO_2 nanoparticle from combine extract of onion and garlic peel. J King Saud Univ 2023;35(8):102918. https://doi.org/10.1016/j.jksus.2023.102918.
[54] Khamis M, Gouda GA, Nagiub AM. Green synthesis of zinc oxide nanoparticles: Characterization, organic dye degradation and evaluation of their antibacterial activity. Al-Azhar Bull Sci 2023;34(2):7. https://doi.org/10.58675/2636-3305.1650.
[55] Hasanin MS, Hashem AH, Al-Askar AA, et al. A novel nanocomposite based on mycosynthesized bimetallic zinc-copperoxide nanoparticles, nanocellulose and chitosan: Characterization, antimicrobial and photocatalytic activities. Electron J Biotechnol 2023;65:45–55. https://doi.org/10.1016/j.ejbt.2023.05.001.
[56] Fouda A, Eid AM, Abdelkareem A, et al. Phyco-synthesized zinc oxide nanoparticles using marine macroalgae, *Ulva fasciata* Delile, characterization, antibacterial activity, photocatalysis, and tanning wastewater treatment. Catalysts 2022;12(7):756. https://doi.org/10.3390/catal12070756.
[57] Khalil AM, Saied E, Mekky AE, et al. Green biosynthesis of bimetallic selenium–goldnanoparticles using *Pluchea indica* leaves and their biological applications. Front Bioeng Biotechnol 2024;11:1294170. https://doi.org/10.3389/fbioe.2023.1294170. PMid: 38274007.
[58] Hashem AH, El-Sayyad GS, Al-Askar AA, et al. Watermelon rind mediated biosynthesis of bimetallic selenium-silver nanoparticles: Characterization, antimicrobial and anticancer activities. Plants 2023;12(18):3288. https://doi.org/10.3390/plants12183288. PMid: 37765453.
[59] Hashem AH, Al-Askar AA, Saeb MR, et al. Sustainable biosynthesized bimetallic ZnO@SeO nanoparticles from pomegranate peel extracts: Antibacterial, antifungal and anticancer activities. RSC Adv 2023;13:22918–27. https://doi.org/10.1039/D3RA03260D. PMid: 37520090.
[60] Selim S, Almuhayawi MS, Saddiq AA, et al. Synthesis of novel MgO-ZnO nanocomposite using *Pluchea indica* leaf extract and study of their biological activities. Bioresour Bioprocess 2025;12:33. https://doi.org/10.1186/s40643-025-00848-x. PMid: 40220116.
[61] Hashem AH, Rizk SH, Abdel-Maksoud MA, et al. Unveiling anticancer, antimicrobial, and antioxidant activities of novel synthesized bimetallic

boron oxide–zinc oxide nanoparticles. RSC Adv 2023;13:20856–67. https://doi.org/10.1039/D3RA03413E. PMid: 37448639.
[62] Elkady FM, Hashem AH, Salem SS, et al. Unveiling biological activities of biosynthesized starch/silver-selenium nanocomposite using *Cladosporium cladosporioides* CBS 174. BMC Microbiol 2024;24:78. https://doi.org/10.1186/s12866-024-03228-1. PMid: 38459502.
[63] Lee G, Lee YJ, Kim Y-J, et al. Synthesis of Au–Ag bimetallic nanoparticles using Korean red ginseng (*Panax ginseng Meyer*) root extract for chemo-photothermal anticancer therapy. Arch Pharm Res 2023;46:659–78. https://doi.org/10.1007/s12272-023-01457-y. PMid: 37592169.
[64] Elsayed KA, Alomari M, Drmosh QA, et al. Fabrication of ZnO-Ag bimetallic nanoparticles by laser ablation for anticancer activity. Alex Eng J 2022;61:1449–57. https://doi.org/10.1016/j.aej.2021.06.051.
[65] Austin J, Minelli C, Hamilton D, et al. Nanoparticle number concentration measurements by multi-angle dynamic light scattering. J Nanopart Res 2020;22:108. https://doi.org/10.1007/s11051-020-04840-8.
[66] Rohmah M, Raharjo S, Hidayat C, et al. Application of response surface methodology for the optimization of β-carotene-loaded nanostructured lipid carrier from mixtures of palm stearin and palm olein. J Am Oil Chem Soc 2020;97(2):213–23. https://doi.org/10.1002/aocs.12310.
[67] Nwozo OS, Magdalene EE, Maduabuchi AP, et al. Antioxidant, phytochemical, and therapeutic properties of medicinal plants: A review. Int J Food Prop 2023;26:359–88. https://doi.org/10.1080/10942912.2022.2157425.
[68] Sun W, Shahrajabian MH. Therapeutic potential of phenolic compounds in medicinal plants—Natural health products for human Health. Molecules 2023;28(4):1845. https://doi.org/10.3390/molecules28041845. PMid: 36838831.
[69] Villagrán Z, Anaya-Esparza LM, Velázquez-Carriles CA, et al. Plant-based extracts as reducing, capping, and stabilizing agents for the green synthesis of inorganic nanoparticles. Resources 2024;13(6):70. https://doi.org/10.3390/resources13060070.
[70] Jeevanandam J, Kiew SF, Boakye-Ansah S, et al. Green approaches for the synthesis of metal and metal oxide nanoparticles using microbial and plant extracts. Nanoscale 2022;14:2534–71. https://doi.org/10.1039/D1NR08144F. PMid: 35133391.
[71] El-Amier YA, Abduljabbar BT, El-Zayat MM, et al. Biosynthesis of metal/metal oxide nanoparticles via *Deverra tortuosa*: Characterization, GC/MS profiles, and biological potential. Sci Rep 2024;14:23522. https://doi.org/10.1038/s41598-024-74471-9. PMid: 39384959.
[72] Anjum S, Nawaz K, Ahmad B, et al. Green synthesis of biocompatible core–shell (Au–Ag) and hybrid (Au–ZnO and Ag–ZnO) bimetallic nanoparticles and evaluation of their potential antibacterial, antidiabetic, antiglycation and anticancer activities. RSC Adv 2022;12:23845–59. https://doi.org/10.1039/D2RA03196F PMid:3 6093232.
[73] Vorontsov AV, Tsybulya SV. Influence of nanoparticles size on XRD patterns for small monodisperse nanoparticles of Cu^0 and TiO_2 anatase. Ind Eng Chem Res 2018;57(7):2526–36. https://doi.org/10.1021/acs.iecr.7b04480.
[74] Nadjia L, Abdelkader E. Design, synthesis and characterization of ceria: Assessment of crystallite size and intrinsic strain using XRD profile analysis and its photocatalytic applications. J Iran Chem Soc 2025;22:297–324. https://doi.org/10.1007/s13738-024-03149-w.
[75] Shekhar S, Singh S, Gandhi N, et al. Green chemistry based benign approach for the synthesis of titanium oxide nanoparticles using extracts of *Azadirachta indica*. Cleaner Eng Technol 2023;13:100607. https://doi.org/10.1016/j.clet.2023.100607.
[76] Asaulyuk T, Saribyekova Y, Semeshko O, et al. Synthesis and structural characterization of ZnO nanoparticles. Herald Khmelnytskyi Natl Univ 2022;311:35–41. https://doi.org/10.31891/2307-5732-2022-311-4-35-41.
[77] Modi S, Fulekar MJ. Green synthesis of zinc oxide nanoparticles using garlic skin extract and its characterization. J Nanostruct 2020;10(1):20–7. https://doi.org/10.22052/JNS.2020.01.003.
[78] Masud S, Munir H, Irfan M, et al. *Allium cepa*-based zinc oxide nanoparticles: Characterization and biochemical potentials. Bioinspired Biomim Nanobiomater 2023;12(2):82–93. https://doi.org/10.1680/jbibn.22.00038.
[79] Kaabo HE, Saied E, Hassan SD, et al. *Penicillium oxalicum*-mediated the green synthesis of silica nanoparticles: Characterization and environmental applications. Biomass Convers Biorefin 2024;15:5229–46. https://doi.org/10.1007/s13399-024-05350-6.
[80] Qiang ZX, Hong YL, Meng T, et al. ZnO, TiO_2, SiO_2, and Al_2O_3 nanoparticles-induced toxic effects on human fetal lung fibroblasts. Biomed Environ Sci 2011;24(6):661–9. https://doi.org/10.3967/0895-3988.2011.06.011.
[81] Rashid F, Pervaiz I, Malik H, et al. Investigations on synergistic and antioxidant actions of medicinal plant-based biosynthesis of zinc oxide nanoparticles against *E. coli* and *K. pneumonia* bacteria. Comb Chem High Throughput Screen 2022;25(7):1200–6. https://doi.org/10.2174/1386207324666210302102111. PMid: 33653240.
[82] Rajashekara S, Shrivastava A, Sumhitha S, et al. Biomedical applications of biogenic zinc oxide nanoparticles manufactured from leaf extracts of *Calotropis gigantea* (L.) Dryand. BioNanoScience 2020;10:654–71. https://doi.org/10.1007/s12668-020-00746-w.
[83] Maduabuchi E, Siwe-Nound X. Green synthesis of zinc oxide nanoparticles and their antibiotic-potentiation activities of mucin against pathogenic bacteria. Res J Nanosci Nanotechnol 2020;10:9–14. https://doi.org/10.3923/rjnn.2020.9.14.
[84] Nachimuthu S, Thangamani C, Thiyagarajulu N, et al. Facile synthesis of ZnO-Y_2O_3 nanocomposite for photocatalytic and biological applications. Catal Commun 2023;184:106786. https://doi.org/10.1016/j.catcom.2023.106786.
[85] Elkady FM, Badr BM, Saied E, et al. Green biosynthesis of bimetallic copper oxide-selenium nanoparticles using leaf extract of *Lagenaria siceraria*: Antibacterial, anti-virulence activities against multidrug-resistant *Pseudomonas aeruginosa*. Int J Nanomed 2025;20:4705–27. https://doi.org/10.2147/IJN.S497494. PMid: 40255676.
[86] Kamel Z, Helmy NA, Soliman MK, et al. Impact of biofilm production in methicillin resistant Staphylococcus aureus among diabetic foot patient. Egypt J Med Microbiol 2018;27:93–8. https://doi.org/10.21608/ejmm.2018.285547.
[87] Anupong W, On-uma R, Jutamas K, et al. Antibacterial, antifungal, antidiabetic, and antioxidant activities potential of *Coleus aromaticus* synthesized titanium dioxide nanoparticles. Environ Res 2023;216(Part 3):114714. https://doi.org/10.1016/j.envres.2022.114714. PMid: 36334834.
[88] Chemingui H, Moulahi A, Missaoui T, et al. A novel green preparation of zinc oxide nanoparticles with *Hibiscus sabdariffa* L.: Photocatalytic performance, evaluation of antioxidant and antibacterial activity. Environ Technol 2024;45(5):926–44. https://doi.org/10.1080/09593330.2022.2130108. PMid: 36170044.
[89] Shivalingam C, Gurumoorthy K, Murugan R, et al. Herbal-based green synthesis of TB-ZnO-TiO (II) nanoparticles composite from *Terminalia bellirica*: Characterization, toxicity assay, antioxidant assay, and antimicrobial activity. Cureus 2024;16(3):e55686. https://doi.org/10.7759/cureus.55686. PMid: 38586786.
[90] Bai Q, Zhang Y, Cai R, et al. AMP-Coated TiO_2 doped ZnO nanomaterials enhanced antimicrobial activity and efficacy in otitis media treatment by elevating hydroxyl radical levels. Int J Nanomed 2024;19:2995–3007. https://doi.org/10.2147/IJN.S449888. PMid: 38559446.
[91] Pauzi N, Zain NM, Kutty RV, et al. Antibacterial and antibiofilm properties of ZnO nanoparticles synthesis using gum arabic as a potential new generation antibacterial agent. Mater Today Proc 2021;41(Part 1):1–8. https://doi.org/10.1016/j.matpr.2020.06.359.
[92] Yeroslavsky G, Lavi R, Alishaev A, et al. Sonochemically-produced metal-containing polydopamine nanoparticles and their antibacterial and antibiofilm activity. Langmuir 2016;32(20):5201–12. https://doi.org/10.1021/acs.langmuir.6b00576. PMid: 27133213.
[93] Wong CW, Chan YS, Jeevanandam J, et al. Response surface methodology optimization of mono-dispersed MgO nanoparticles fabricated by ultrasonic-assisted sol–gel method for outstanding antimicrobial and antibiofilm activities. J Clust Sci 2020;31:367–89. https://doi.org/10.1007/s10876-019-01651-3.
[94] Doğan SŞ, Kocabaş A. Green synthesis of ZnO nanoparticles with *Veronica multifida* and their antibiofilm activity. Hum Exp Toxicol 2020;39(3):319–27. https://doi.org/10.1177/0960327119888270. PMid: 31726879.
[95] Masoudi M, Mashreghi M, Zenhari A, et al. Combinational antimicrobial activity of biogenic TiO_2 NP/ZnO NPs nanoantibiotics and amoxicillin-clavulanic acid against MDR-pathogens. Int J Pharm 2024;652:123821. https://doi.org/10.1016/j.ijpharm.2024.123821. PMid: 38242259.
[96] Jin Y, Li B, Saravanakumar K, et al. Phytogenic titanium dioxide (TiO_2) nanoparticles derived from *Rosa davurica* with anti-bacterial and anti-biofilm activities. J Clust Sci 2022;33:1435–43. https://doi.org/10.1007/s10876-021-02024-5.
[97] Fatima S, Ali K, Ahmed B, et al. Titanium dioxide nanoparticles Induce inhibitory effects against planktonic cells and biofilms of human oral cavity isolates of *Rothia mucilaginosa, Georgenia* sp and *Staphylococcus saprophyticus*. Pharmaceutics 2021;13(10):1564. https://doi.org/10.3390/pharmaceutics13101564. PMid: 34683856.
[98] Dan S, Khan S. Green coalescence and characterization of TiO_2 nanoparticles and evaluation of its antibiofilm activity. Rasayan J Chem 2019;12(4):2252–9. https://doi.org/10.31788/RJC.2019.1245341.
[99] Aljabali AA, Obeid MA, Bakshi HA, et al. Synthesis, characterization, and assessment of anti-cancer potential of ZnO nanoparticles in an *in vitro* model of breast cancer. Molecules 2022;27(6):1827. https://doi.org/10.3390/molecules27061827. PMid: 35335190.
[100] Lotfian H, Nemati F. Cytotoxic effect of TiO_2 nanoparticles on breast cancer cell line (MCF-7). IIOAB J 2016;7(Supp 4):219–24.
[101] Gong L, Tang Y, An R, et al. RTN1-C mediates cerebral ischemia/reperfusion injury via ER stress and mitochondria-associated apoptosis pathways. Cell Death Dis 2017;8:e3080. https://doi.org/10.1038/cddis.2017.465. PMid: 28981095.
[102] Onodera R, Jimma Y, Suzuki A, et al. The regulation pathway of VEGF gene expression is different between 2D cells and 3D spheroids in human lung cancer cells. Biol Pharm Bull 2023;46(4):608–13. https://doi.org/10.1248/bpb.b22-00772. PMid: 37005305.
[103] Amirchaghmaghi E, Rezaei A, Moini A, et al. Gene expression analysis of VEGF and its receptors and assessment of its serum level in unexplained recurrent spontaneous abortion. Cell J (Yakhteh) 2015;16(4):538–45. https://doi.org/10.22074/cellj.2015.498. PMid: 25685744.